



ORIGINAL ARTICLE

Obesity Biology and Integrated Physiology

The role of adipogenic capacity and dysfunctional subcutaneous adipose tissue in the inheritance of type 2 diabetes mellitus: cross-sectional study

Michaela Šiklová^{1,2}  | Veronika Šrámková^{1,2} | Michal Koc^{1,2} |
 Eva Krauzová^{1,2,3} | Terezie Čížková¹  | Barbora Ondrůjová¹ | Marek Wilhelm¹ |
 Zuzana Varaliová¹ | Ondrej Kuda⁴ | Jana Neubert¹ | Lukáš Lambert⁵ |
 Moustafa Elkalaf¹ | Jan Gojda^{2,3} | Lenka Rossmeislová^{1,2}

¹Department of Pathophysiology, Center for Research on Nutrition, Metabolism and Diabetes, Third Faculty of Medicine, Charles University, Prague, Czech Republic

²Franco-Czech Laboratory for Clinical Research on Obesity, Third Faculty of Medicine, Charles University, Prague, Czech Republic

³Department of Internal Medicine, Královské Vinohrady University Hospital, Prague, Czech Republic

⁴Institute of Physiology, Czech Academy of Sciences, Prague, Czech Republic

⁵Department of Radiology, First Faculty of Medicine, Charles University and General University Hospital, Prague, Czech Republic

Correspondence

Michaela Šiklová, Department of Pathophysiology, Third Faculty of Medicine, Charles University, Ruska 87, 100 00 Prague 10, Czech Republic.
 Email: michaela.siklova@lf3.cuni.cz

Funding information

Ministry of Health of the Czech Republic, Grant/Award Number: NV19-01-00263; Czech Academy of Sciences, Grant/Award Number: LQ200111901; European Union - Next Generation EU, Grant/Award Number: LX22NPO5104; Grant Agency of the Czech Republic, Grant/Award Number: 16-14048S; Charles University, Grant/Award Numbers: 260646/SVV/2023, COOPERATIO

Abstract

Objective: This study tested the hypothesis that limited subcutaneous adipose tissue (SAT) expansion represents a primary predisposition to the development of type 2 diabetes mellitus (T2DM), independent of obesity, and identified novel markers of SAT dysfunction in the inheritance of T2DM.

Methods: First-degree relatives (FDR) of T2DM patients ($n = 19$) and control individuals ($n = 19$) without obesity (fat mass < 25%) were cross-sectionally compared. Body composition (bioimpedance, computed tomography) and insulin sensitivity (IS; oral glucose tolerance test, clamp) were measured. SAT obtained by needle biopsy was used to analyze adipocyte size, lipidome, mRNA expression, and inflammatory markers. Primary cultures of adipose precursors were analyzed for adipogenic capacity and metabolism.

Results: Compared with control individuals, FDR individuals had lower IS and a higher amount of visceral fat. However, SAT-derived adipose precursors did not differ in their ability to proliferate and differentiate or in metabolic parameters (lipolysis, mitochondrial oxidation). In SAT of FDR individuals, lipidomic and mRNA expression analysis revealed accumulation of triglycerides containing polyunsaturated fatty acids and increased mRNA expression of lysyl oxidase (LOX). These parameters correlated with IS, visceral fat accumulation, and mRNA expression of inflammatory and cellular stress genes.

Conclusions: The intrinsic adipogenic potential of SAT is not affected by a family history of T2DM. However, alterations in LOX mRNA and polyunsaturated fatty acids in triacylglycerols are likely related to the risk of developing T2DM independent of obesity.

This is an open access article under the terms of the [Creative Commons Attribution](https://creativecommons.org/licenses/by/4.0/) License, which permits use, distribution and reproduction in any medium, provided the original work is properly cited.

© 2024 The Authors. *Obesity* published by Wiley Periodicals LLC on behalf of The Obesity Society.

INTRODUCTION

It is estimated that 463 million people worldwide had type 2 diabetes mellitus (T2DM) in 2019, and this number is expected to rise to 700 million in just 25 years [1]. An individual's risk of developing T2DM results from a combination of genetic predisposition and environmental factors. Heredity plays an important role in the development of T2DM because first-degree relatives (FDR) have higher incidence (hazard ratio 2.44, 95% confidence interval [CI]: 2.03–2.95) of the disease than individuals with no family history of diabetes, regardless of body mass index (BMI), waist circumference, and other risk factors [2]. However, the majority (85%–90%) of patients with T2DM also have overweight or obesity [3], which makes the presence of overweight/obesity another important risk factor for the development of diabetes.

The accumulation of adipose tissue (AT) in obesity is often associated with its hypertrophy leading to dysfunction. Hypertrophied adipocytes exhibit lower insulin sensitivity (IS), higher basal lipolysis, and increased production of inflammatory cytokines that contribute to the development of low-grade chronic inflammation [4]. AT hypertrophy is also associated with immune cell accumulation and fibrosis [5], as well as with lipid accumulation and lipotoxicity in other tissues [6, 7]. All of these features of hypertrophied AT are associated with the development of insulin resistance (IR) and subsequent diabetes in individuals with obesity. Nevertheless, findings that have supported the theory of AT dysfunction in hypertrophic obesity are mostly derived from murine models, whereas human data are much scarcer and the level of evidence a lot weaker. In humans, hypertrophic subcutaneous AT (SAT) was found in individuals diagnosed with impaired glucose tolerance and T2DM [8, 9], as well as in individuals with a genetic predisposition to T2DM who do not have obesity [5, 10, 11]. The main cause of SAT hypertrophy in these individuals is thought to be a reduced ability of adipocyte precursors (APCs) to differentiate into new metabolically healthy adipocytes [6, 12], i.e., reduced SAT hyperplastic expandability [13]. Indeed, it has been shown that limited adipogenic capacity of APCs is present in individuals with T2DM [14] and in FDR individuals [15, 16]. One important contributor to limited ability of adipocytes to differentiate in these individuals was senescent phenotype of APCs [15, 16]. However, predisposed individuals in previous studies have already had slightly increased amounts of fat, which may mask the primary cause of hypertrophy and reduced adipogenic capacity in these people.

Therefore, in this study, we tested whether the limited hyperplastic expandability is indeed present before the fat accumulates in FDR individuals, i.e., whether it is a primary inherited feature. We also focused on other characteristics of dysfunctional SAT such as a proinflammatory state, altered immune cell profile, fibrosis, senescence, and impaired metabolic activity (lipolysis, lipogenesis), which might strongly affect a differentiation of new adipocytes. We analyzed whether these SAT characteristics were related to the observed *in vivo* phenotype of our participants, specifically measures of adiposity, IS, and glucose homeostasis.

Study Importance

What is already known?

- Hypertrophy of subcutaneous adipose tissue (SAT) is found not only in individuals with obesity but also in individuals with a family predisposition to type 2 diabetes mellitus (T2DM) without obesity and is associated with unfavorable metabolic phenotype and insulin resistance.
- It is uncertain whether the primary cause of SAT hypertrophy in relatives of patients with T2DM prior to the fat mass accumulation is limited adipogenic capacity or whether there is another cause of SAT dysfunction in these individuals.

What does this study add?

- *In vitro* adipogenic potential and metabolism of adipose cells are not impaired by family predisposition to T2DM in lean male individuals.
- Increase in triglycerols containing polyunsaturated fatty acids and (lysyl oxidase) LOX mRNA is present in male first-degree relatives and is associated with visceral fat accumulation and insulin resistance, as well as with inflammatory and cellular stress genes in SAT.

How might these findings change the direction of research or the focus of clinical practice?

- Our findings suggest that there are functional changes in SAT in lean individuals who are predisposed to T2DM that are not primarily related to limited adipogenic capacity but reveal new pathways for further research into the pathophysiology and treatment of T2DM.

METHODS

Participants and design

Male individuals without obesity (BMI, 20–30 kg/m²; age, 25–45 years) were recruited according to the family history of T2DM into two groups: 1) FDR individuals of patients with T2DM; and 2) control group (CON), i.e., individuals without any family history of T2DM. A total of 51 male individuals were evaluated for compliance with the inclusion and exclusion criteria (see [online Supporting Information Methods](#)). Based on medical history and laboratory findings, 38 eligible participants (Figure 1; FDR [*n* = 19], CON [*n* = 19]) were considered as generally healthy, except for several cases of impaired fasting glucose and impaired glucose tolerance (CON [*n* = 3]; FDR [*n* = 4]). The groups did not differ in BMI, fat mass (FM), or age (Table 1). Importantly, the presence of impaired fasting glucose or impaired glucose tolerance in both

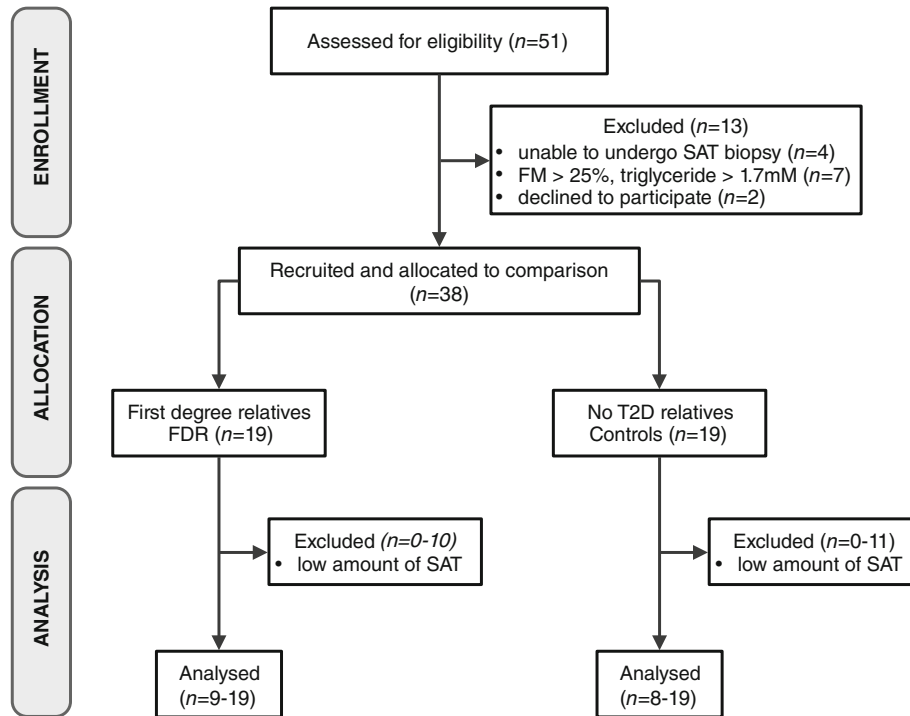


FIGURE 1 Flow diagram of study design. FDR, first-degree relative; FM, fat mass; SAT, subcutaneous adipose tissue; T2D, type 2 diabetes mellitus.

TABLE 1 Anthropometric and biochemical characteristics of CON and FDR participants

	CON (n = 19)	FDR (n = 19)	p value
Age (y)	35 ± 4	35 ± 5	0.868
Weight (kg)	81.9 ± 9.5	84.4 ± 6.6	0.297
BMI (kg/m ²)	24.6 ± 2.0	25.6 ± 2.2	0.147
Waist circumference (cm)	84.4 ± 5.4	86.4 ± 6.6	0.325
FM (%)	16.7 ± 3.9	18.7 ± 3.8	0.124
FFM (kg)	68.0 ± 7.2	68.5 ± 4.3	0.797
SAT (mL)	318 ± 180 ^b	380 ± 135 ^a	0.264
VAT (mL)	176 ± 98 ^b	292 ± 172 ^a	0.020
SAT/VAT ratio	1.99 ± 0.94 ^b	1.54 ± 0.57 ^a	0.080
TAG (mmol/L)	0.90 ± 0.41	0.94 ± 0.42	0.780
HDL (mmol/L)	1.35 ± 0.28	1.33 ± 0.30	0.807
Cholesterol (mmol/L)	4.32 ± 0.70	4.70 ± 0.88	0.164

Note: Data are expressed as mean ± SD; p value: unpaired t test (data were log-transformed when needed, based on Shapiro–Wilk normality test).

Abbreviations: CON, control; FDR, first-degree relative; FFM, fat-free mass; FM, fat mass; HDL, high-density lipoprotein; SAT, subcutaneous adipose tissue; TAG, triglyceride; VAT, visceral adipose tissue.

^aClinical variable was measured in 16 patients.

^bClinical variable was measured in 18 patients.

groups of participants did not affect the overall results of the study (Figures S1–S4). All procedures were in accordance with the 1964 Declaration of Helsinki and were approved by ethics committee of

the Third Faculty of Medicine, Charles University and Královské Vinohrady University Hospital (Prague, Czech Republic). Informed consent was obtained from all participants included in the study. Trial registration number is NCT03155412 ([ClinicalTrials.gov](https://clinicaltrials.gov)).

Clinical investigations

Anthropometric measurements, blood sampling, and needle biopsy of SAT were performed after overnight fast, as previously described [17]. A 2-h oral glucose tolerance test (OGTT) was performed with a 75-g glucose drink, and IS indices, namely the Matsuda and Stumvoll indices [18, 19], were calculated. The hyperinsulinemic-euglycemic clamp was performed as described [17]. Glucose disposal was calculated from the last 30-min steady-state glucose infusion rate (glucose disposal, corrected for body fat-free mass [FFM] = milligrams of infused glucose per kilograms of FFM per minute; metabolic clearance = M-value per mean glucose in steady state × [100/18] [milliliters per kilograms per minute]). In the majority of participants (CON [n = 18]; FDR [n = 16]), computed tomography scanning for the evaluation of visceral AT (VAT) and SAT volume was performed as described previously [20].

SAT sample processing

The samples of SAT (2–3 g) were aseptically washed with phosphate-buffered saline (PBS)/gentamicin, cleaned from blood vessels and fibrous material, and divided into aliquots: ~300 mg were snap-frozen

in aliquots in liquid nitrogen and then stored at -80°C until subsequent analyses (lipidomics, mRNA expression), and ~ 2 g were minced and digested by collagenase for isolation of adipocytes and stromal vascular fraction (SVF) cells (including preadipocytes and immune cells) [17]. SVF cells were used for cell culture establishment and flow cytometry analysis. In a subgroup of participants (CON [$n = 13$]; FDR [$n = 12$]), explants of SAT (~ 300 mg) and SAT lysates were prepared (online Supporting Information Methods). Owing to the limited volume of SAT obtained by needle biopsy or due to technical reasons imposed by the methodology, different numbers of SAT samples were analyzed by each technique (CON [$n = 8-19$]; FDR [$n = 9-19$]; exact numbers are given for each analysis/figure).

Adipocyte size

The adipocytes isolated by collagenase digestion were separated by centrifugation (300 g/10 min) and transferred to the 1% bovine serum albumin (BSA)/PBS solution (1:1) with methylene blue. Images of the adipocyte suspension were captured by fully inverted automated research microscope Leica DMI 6000 CS with attached monochrome camera Leica DFC 350 FX on right port. The pictures were acquired by bright field 10×0.3 DRYobjective via software Leica LAS AF 2.7.2. For each participant, three images were taken (on average, 350 adipocytes/picture) and analyzed using the software CellProfiler combined with an in-house program designed to distinguish adipocytes from free lipid droplets. Relative frequency (percentage), which reflects the fraction of adipocytes in different size groups, was calculated using frequency distribution analysis (GraphPad Prism software), when bin width was set to $10 \mu\text{m}$ and the range of size was 15 to $145 \mu\text{m}$. Adipocytes smaller than $15 \mu\text{m}$ or larger than $145 \mu\text{m}$ were excluded from the analysis due to the very small number of cells with this diameter.

Primary preadipocyte proliferation and differentiation

SVF cells after collagenase digestion were cultivated in proliferation medium (composition in online Supporting Information Methods) upon 70% confluence and passed twice prior cryopreservation. For proliferation testing, WST-1 assay and sensitivity of preadipocytes to proliferation stimuli (fetal bovine serum, FBS) was applied (Supporting Information Methods).

For differentiation, cells were plated in the density of 10,000 cells/ cm^2 and allowed to grow until they were 2-days postconfluent, and then the differentiation was started by adipogenesis induction media (online Supporting Information Methods). After 6 days, an adipogenesis maintenance medium was used (Supporting Information Methods) until day 12. The level of differentiation was analyzed by Oil Red O (ORO) staining and mRNA expression.

Analysis of insulin signaling, lipolytic assay, and Western blot were performed as described in online Supporting Information Methods.

Seahorse measurement

The oxygen consumption rate was measured in a subgroup of participants (CON [$n = 8$]; FDR [$n = 9$]). Preparation of cells and setting of the experiment are described in online Supporting Information Methods. To analyze individual inputs of glucose and fatty acids, cells were treated with etomoxir (inhibitor of carnitine palmitoyltransferase-1) or UK5099 (inhibitor of the mitochondrial pyruvate transporter).

Flow cytometry analysis of immune cell populations

Collected SVF cells were stained with the antibodies and analyzed on BD FACSVerser flow cytometer and by BD FACSuite Software 1.0.6 (BD Biosciences). The set of antibodies is listed in online Supporting Information Methods. The number of immune cells in the analyzed populations was expressed as a percentage of gated events related to $\text{CD}45^+/\text{CD}14^+$ (monocytes/macrophages) and $\text{CD}3^+/\text{CD}4^+$ (lymphocytes) positive events. The gating strategy and description of cell populations were similar as described [17].

Untargeted lipidomics

Extraction of SAT samples (~ 20 mg) was performed by a biphasic solvent system of cold methanol, methyl tert-butyl ether, and water [21]. The liquid chromatography-mass spectrometry analysis consisted of a Vanquish UHPLC System (Thermo Fisher Scientific) coupled to a Q Exactive Plus mass spectrometer (Thermo Fisher Scientific) and UltiMate 3000 RSLC UHPLC system coupled to a QTRAP 5500/SelexION mass spectrometer (SCIEX) [21].

Gene expression analysis

RNA isolation and transcription was performed as described in online Supporting Information Methods. All of the samples were measured in technical duplicates, and the biological replicates for each analysis are listed in figure legends. For microfluidics, 4 ng of complementary DNA was pre-amplified within 16 cycles. TaqMan gene expression assays of all target genes (Tables S1-S3) were pooled together and diluted with water to the final concentration of $0.2 \times$ for each probe. The real-time quantitative polymerase chain reaction was performed in duplicates on Biomark real-time quantitative polymerase chain reaction system using a 96×96 array (Fluidigm) or on sequence detection system (ABI PRISM 7500; Applied Biosystems). Data were normalized to the reference gene TATA box binding protein (TBP), and the relative expression was calculated as $2^{-\Delta\text{Ct}}$ and $2^{-\Delta\Delta\text{Ct}}$.

Analyses of plasma, AT lysates, and conditioned media are described in online Supporting Information Methods.

Statistical analysis

Data were analyzed using GraphPad Prism version 9.2.0 and 10.1.0 software. Data are presented as mean \pm SD or SEM or as median with interquartile range (IQR) (mRNA expression). The analysis was performed in eight to nineteen CON and nine to nineteen FDR participants based on availability and/or quality control of the samples and outlier analysis (ROUT method, Q 0.1%). Differences between CON and FDR groups were analyzed by two-tailed unpaired t test, and data were log-transformed for analysis when needed (based on Shapiro–Wilk normality test). The data sets of mRNA gene expression were analyzed by multiple Mann–Whitney tests with two stage step-up method of Benjamini, Krieger, and Yekutieli (FDR $<$ 0.05). Correlations are expressed by Pearson's correlation coefficient. Lipidomic data set was processed in MetaboAnalyst as described previously [21]. The level of significance was set at $p <$ 0.05; q value (false discovery rate-adjusted p value) $<$ 0.05.

RESULTS

Family predisposition to T2DM affects IS and amount of visceral fat

CON and FDR participants did not differ in most anthropometric and biochemical parameters; however, FDR participants showed higher amounts of VAT (Table 1). FDR individuals also had higher fasting glucose levels and lower IS as assessed by the Matsuda and Stumvoll indices (Table 2), whereas glucose disposal, corrected for FFM; metabolic clearance; and the AT insulin resistance index (Adipo-IR) values did not differ between the groups. There was no significant difference in the mean size of isolated adipocytes between the groups (CON [70.9 \pm 2.7]; FDR [70.7 \pm 2.9] μ m). Although the distribution of adipocyte sizes was also similar, a trend to higher relative frequency of large hypertrophied adipocytes (130 \pm 5 μ m; $p =$ 0.06) and lower relative frequency of medium-size adipocytes (80 \pm 5 μ m) in FDR participants ($p =$ 0.06; Figure 2B) was present. In the entire cohort, large adipocytes (95–145 μ m) correlated positively with waist circumference, FM, amount of SAT and VAT, lipid parameters, and plasma leptin levels and correlated negatively with some IS indices. Small-to-average adipocytes (35–85 μ m) had an opposite correlation pattern (Figure 2C).

Proinflammatory and the fibrotic microenvironment plays an important role in pathogenesis of T2DM [5, 22]. Therefore, we analyzed composition of immune cells and markers of inflammation and fibrosis in SAT. Our data show higher relative content of C-C chemokine receptor type 2 (CCR2)-positive macrophages in FDR participants, whereas other immune cells populations were not different between FDR and CON participants (Figure 2D). The levels of hydroxyproline, a surrogate measure of fibrosis, and levels of several soluble markers of fibrosis and cytokines (Figure 2E,F) in media conditioned by SAT explants did not differ between groups. In the entire cohort, the interleukin 6 (IL-6) secreted by SAT correlated with waist circumference, amount of VAT and SAT, and relative number of large

TABLE 2 Parameters of IS, glucose homeostasis, and adipokines in CON and FDR participants

	CON (n = 19)	FDR (n = 19)	<i>p</i> value
Glucose (mmol/L)	5.27 \pm 0.46	5.52 \pm 0.33	0.048
Insulin (mU/L)	5.11 \pm 2.80	7.39 \pm 4.38	0.064
FFA (mmol/L)	1.09 \pm 0.47	0.97 \pm 0.33	0.369
HOMA-IR	1.22 \pm 0.73	1.81 \pm 1.06	0.075
AUC Ins _{OGTT}	4108 \pm 1587	4830 \pm 2444	0.287
AUC Glu _{OGTT}	189 \pm 98	174 \pm 66	0.581
Insulin _{OGTT 120min} (mU/L)	21.6 \pm 10.9	34.6 \pm 20.4	0.019
Insulin _{HIC 120min} (mU/L)	68.2 \pm 15.9	67.1 \pm 20.5	0.850
Matsuda index	8.35 \pm 3.99	6.12 \pm 2.77	0.043
Stumvoll index	0.114 \pm 0.009	0.105 \pm 0.013	0.019
MCR _{glu} (mL/kg/min)	8.03 \pm 2.90	7.41 \pm 2.41	0.476
M _{FFM} (mg/kg/min)	7.95 \pm 2.14	7.65 \pm 2.43	0.689
Adipo-IR	5.6 \pm 4.6	7.5 \pm 5.9	0.293
Adiponectin (μ g/mL)	3.52 \pm 1.31	2.99 \pm 1.73	0.118
Leptin (ng/mL)	2.90 \pm 1.82	4.00 \pm 3.49	0.280

Note: Data are expressed as mean \pm SD; p value: unpaired t test (data were log-transformed for analysis when needed, based on Shapiro–Wilk normality test).

Abbreviations: Adipo-IR, adipose tissue insulin resistance index; AUC, area under the curve; CON, control; FDR, first-degree relative; FFA, free fatty acids; Glu, glucose; HOMA-IR, homeostatic model assessment of insulin resistance; HIC, hyperinsulinemic-euglycemic clamp; Ins, insulin; IS, insulin sensitivity; MCR_{glu}, metabolic clearance of glucose; M_{FFM}, glucose disposal (corrected for body fat-free mass); OGTT, oral glucose tolerance test.

adipocytes (120 μ m; Figure 2G, not shown). Thus, the proportion of SAT hypertrophic adipocytes is related to the proinflammatory characteristics of SAT, which is consistent with previous studies; however, in general, levels of immune/inflammatory state and fibrotic markers were not affected by family predisposition to T2DM.

Intrinsic proliferative and differentiation potential of preadipocytes

To test the hypothesis that intrinsic adipogenic potential of SAT is impaired in FDR individuals, we used an in vitro culture model of primary preadipocytes in which the cells retain donor properties (Figure 3A) [23]. The proliferative capacity did not differ between the preadipocytes of FDR and CON participants (Figure 3B). Also, mRNA expression (97 analyzed genes) showed no substantial difference in the cellular mRNA expression. Only toll-like receptor 4 (TLR4) and integrin subunit β 1 (ITGB1) mRNA were higher in the preadipocytes of FDR participants ($p <$ 0.05; Figure 3C); however, the significance disappeared after multiple testing correction (Table S1). When preadipocytes from both groups of participants were differentiated into adipocytes, they accumulated similar amounts of neutral lipids and

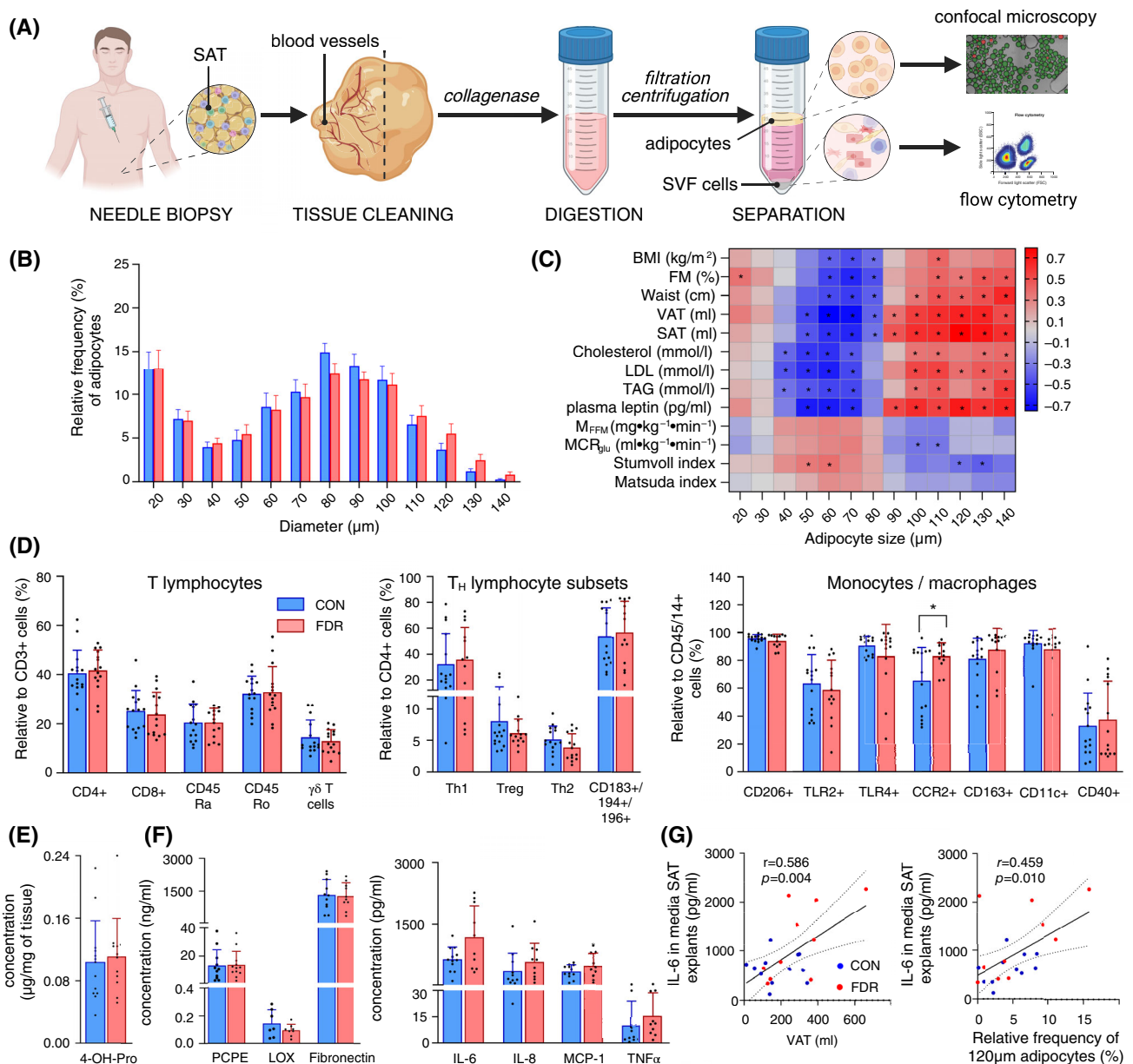


FIGURE 2 Subcutaneous adipose tissue (SAT) characteristics in control (CON) and first-degree relative (FDR) participants. (A) Scheme of sample preparations. (B) Relative frequency of adipocytes in defined size range (bin 10 μm; mean ± SEM, CON [n = 16]; FDR [n = 19], technical triplicates). (C) Correlation of relative frequency of adipocytes with adiposity parameters, lipid profile in plasma, and insulin sensitivity measures (color mapping: Pearson correlation coefficient, *p < 0.05; CON [n = 16]; FDR [n = 19]). (D) Percentage of lymphocyte populations related to CD3+ stromal vascular fraction (SVF) cells in SAT (CON [n = 15]; FDR [n = 14–15]) and percentage of monocyte/macrophage populations related to CD14+ SVF cells in SAT (CON [n = 14–15]; FDR [n = 13–14]). (E) Concentration of factors secreted from SAT explants: procollagen C-endopeptidase enhancer (PCPE), lysyl oxidase (LOX), fibronectin, and cytokines (IL-6, IL-8, monocyte chemoattractant protein-1 [MCP-1], tumor necrosis factor α [TNFα]; CON [n = 8–12]; FDR [n = 10–12], technical duplicates). (G) Correlations of IL-6 secreted by SAT with amount of visceral AT (VAT) and with relative amount of 120 μm adipocytes (Pearson correlation coefficient). Data are expressed as individual points and mean ± SD; *p < 0.05, unpaired t test of log-transformed data. 4-OH-Pro, 4-hydroxyproline. [Color figure can be viewed at wileyonlinelibrary.com]

expressed similar mRNA levels of adipogenic markers (Figure 3D,F, Table S2). Of the genes analyzed (n = 47), perilipin 2 (*PLIN2*), matrix metalloproteinase-2 (*MMP2*), and fibroblast growth factor 1 (*FGF1*) seemed to be elevated in adipocytes of FDR participants

(Figure 3G, Table S2). Interestingly, lipid accumulation in vitro (ORO staining) correlated with proportion of large (110–140 μm) adipocytes in FDR participants, suggesting that the differentiation capacity is diminished in precursors from FDR participants with

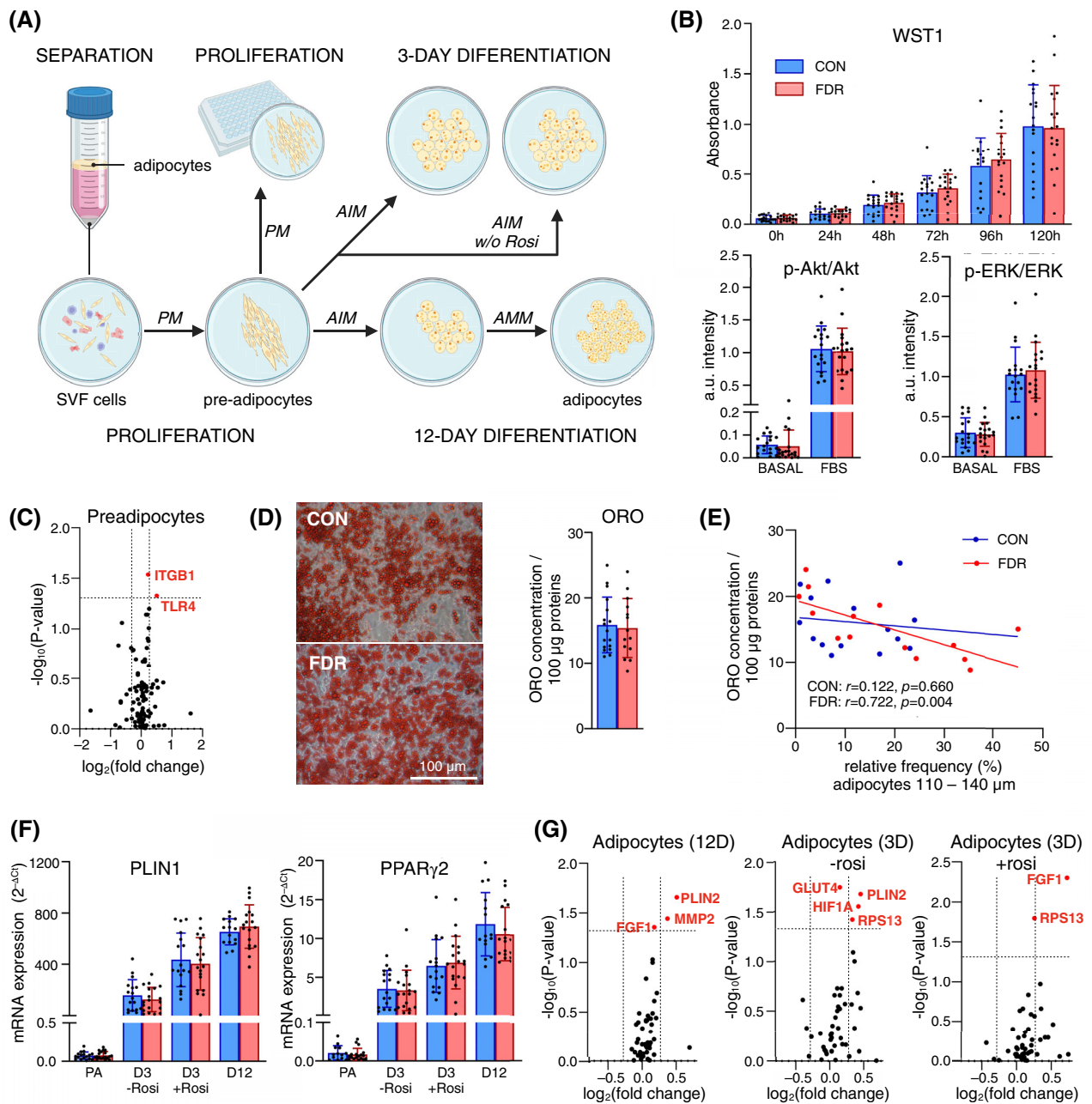


FIGURE 3 Proliferation and differentiation of preadipocytes in vitro. (A) Scheme of primary cell culture setup. (B) Proliferation of preadipocytes: WST-1 assay during 5 days of proliferation (control [CON] [n = 18]; first-degree relative [FDR] [n = 19], technical pentaplicates); phosphorylated-extracellular signal-regulated kinase (ERK/ERK) and phosphorylated-protein kinase B (Akt)/Akt protein expression (Western blot) at baseline and 10 min after FBS stimulation (CON [n = 18]; FDR [n = 19]). (C) Volcano plot of mRNA expression of genes (n = 96) expressed in preadipocytes (PAs), $p < 0.05$ marked in red, Mann-Whitney U test (CON [n = 18]; FDR [n = 19], technical duplicates). (D) Differentiated adipocytes: representative photos of cells stained with Oil Red O (ORO); ORO concentration normalized to protein content (CON [n = 17]; FDR [n = 14], technical triplicates/hexaplicates). (E) Regression analysis of ORO with relative content of large adipocytes (sum of 105–145 µm adipocytes), Pearson correlation coefficient. (F) mRNA expression of selected genes involved in adipogenesis (peroxisome proliferator-activated receptor γ 2 [PPAR γ 2], perilipin [PLIN]) in preadipocytes, early adipocytes exposed to rosiglitazone or not (3 days \pm Rosi), and mature adipocytes (12 days; CON [n = 15–17]; FDR [n = 17–18], technical duplicates). (G) Volcano plot of mRNA expression of genes (n = 46) in early (3 days) and mature (12 days) adipocytes, $p < 0.05$ marked in red, Mann-Whitney U test (CON [n = 15–18]; FDR [n = 17–19], technical duplicates). Data are expressed as individual points and mean \pm SD (WST-1, Western blot, ORO) or median \pm IQR (mRNA expression). SVF, stromal vascular fraction. [Color figure can be viewed at wileyonlinelibrary.com]

already hypertrophic SAT, whereas a similar association was not seen in the CON group (Figure 3E). However, multiple regression analysis did not confirm direct dependence of this association on

diabetes heritability (adipocyte size 110–140: F [1,26] = 7.73, $\beta = -0.1818$, $p = 0.01$; group: F [1,26] = 0.094, $\beta = 0.473$, $p = 0.76$; Figure 3E).

Owing to a presence of rosiglitazone, a peroxisome proliferator-activated receptor γ (*PPAR* γ) agonist and highly potent adipogenic stimulant, in standard adipogenic media could mask subtle differences in the intrinsic adipogenic capacity of cells, we exposed cells to adipogenic medium with and without rosiglitazone for 3 days to follow early steps of adipogenic conversion, which are typically critical for the overall outcome of in vitro adipogenesis. Cells from FDR participants differentiated for 3 days in the absence of rosiglitazone showed higher *PLIN2*, glucose transporter type 4 (*GLUT4*), ribosomal protein S13 (*RPS13*), and hypoxia inducible factor 1 subunit α (*HIF1* α) mRNA levels. Interestingly, *PLIN2* and *FGF1* were increased in cells of FDR participants in both stages of adipogenesis, at 3 and 12 days of differentiation (Figure 3G). However, obtained statistical significances disappeared after correction for multiple testing (Tables S3 and S4). Altogether, cells from FDR participants did not have a significantly reduced ability to proliferate and differentiate into adipocytes in vitro.

Metabolism of in vitro differentiated adipocytes

In in vitro differentiated adipocytes, we investigated metabolic pathways important for healthy AT function, i.e., insulin signaling, lipolytic activity, and mitochondrial respiration (Figure 4). Protein kinase B (Akt) phosphorylation was reduced in cells of FDR participants 5 min after insulin addition, but not after 20 min (Figure 4A), suggesting a delayed insulin signaling response. Lipolytic activity was studied as glycerol release and hormone-sensitive lipase phosphorylation. However, the ability of isoproterenol and 8-bromoadenosine 3',5'-cyclic AMP (8-bromo-cAMP) to induce a lipolytic response and the ability of insulin to suppress this induced lipolysis did not differ between groups (Figure 4B).

To test the mitochondrial metabolism of adipocytes, we analyzed ATP-related respiration and maximal/spare respiratory capacity using substrates from glycolysis or β oxidation (Figure 4C). Input from glycolysis was inhibited by a pyruvate transport inhibitor (UK5099), and, conversely, input from β oxidation was blocked by a long-chain mitochondrial fatty acid transport inhibitor (etomoxir). At the same time, the effect of insulin was studied to stimulate glucose uptake and inhibit potential lipolysis, thereby reducing the intracellular availability of free fatty acids. According to the results, at a basal state, adipocytes use glucose and fatty acids for respiration to a similar extent, whereas, during maximal respiration, these cells rely on pyruvate, irrespective of group (Figure 4D).

Taken together, our data suggest similar metabolic capacity of in vitro differentiated adipocytes from both groups despite a delayed insulin stimulated Akt phosphorylation in FDR participants.

SAT lipid profile and mRNA expression

Because the cells cultured in vitro appear to function well, we decided to gain further insight into SAT metabolic characteristics in vivo. We analyzed the lipid profile and mRNA expression in intact SAT samples.

Lipidomic analysis detected 471 lipid species. Orthogonal Partial least squares - discriminant analysis of these lipid species revealed an apparent separation between the CON and FDR groups (Figure 5A), and variable importance in projection identified 146 discriminating lipid molecules (Table S5). Among the top 20 lipid molecules most differing between the FDR and CON groups, triglycerides containing polyunsaturated fatty acids (PUFA-TAGs) and phospholipids containing saturated or monounsaturated fatty acids (MUFA-PLs) were identified (Figure 5B,C). The levels of PUFA-TAGs were higher and MUFA-PLs lower in FDR participants. Noticeably, in the entire cohort, PUFA-TAGs were positively correlated with the amount of VAT and negatively correlated with the SAT/VAT ratio (Figure 5D). Thus, the amount of PUFA-TAGs in SAT seems to reflect visceral fat accumulation, which is more pronounced in FDR participants. On the other hand, MUFA-PLs (phosphatidylcholine 35:3, phosphatidylethanolamine [PE] 34:2, PE 36:2e) correlated negatively with adiposity (FM, VAT, and SAT), independent of the SAT/VAT ratio (Figure 5D).

In the mRNA expression analysis, 95 genes involved in adipogenesis, lipogenesis, lipolysis, fatty acid, glucose and mitochondrial metabolism, angiogenesis, oxidative stress, inflammation, cell cycle, senescence, and fibrosis were evaluated (Table S6). Significantly upregulated genes in FDR were lysyl oxidase (*LOX*), secreted protein acidic and rich in cysteine (*SPARC*), and *CD36* (Figure 5E), and the trend to increase was observed for cyclin D1 (*CCND1*; $p = 0.06$), with *LOX* being the most important marker ($q = 0.02$).

To investigate the association of these markers with the phenotype of the participants in terms of VAT accumulation and impaired IS, correlations with these parameters were performed. Correlation with the expression of analyzed genes in SAT was also carried out because this could reflect association with dysfunction of AT. Interestingly, *LOX* and *CCND1* mRNA correlated with the amount of VAT, the SAT/VAT ratio, and IS (Matsuda index, M-value; Figure 5F). *LOX* and *CCND1* mRNA correlated strongly together (Figure 5G) and also with mRNA expression of leptin, *SPARC*, *FGF1*, zinc finger matrin-type 3 (*ZMAT3*), and markers of oxidative/cellular stress (NAD(P)H quinone dehydrogenase 1 [*NQO1*], growth differentiation factor 15 [*GDF15*]; Figure 5H,I), and *LOX* mRNA also correlated negatively to MUFA-PLs (Figure 5J). Noticeably, proinflammatory and fibrotic genes in SAT and secretion of proinflammatory cytokines (IL-6, monocyte chemoattractant protein-1) correlated with PUFA-TAGs levels (Figure 5K,L), whereas negative correlation of PUFA-TAGs with metabolic genes was present (Figure 5K). The strongest correlation of PUFA-TAGs was found for *ZMAT3* and *CCND1* (Figure 5K). Together, these findings suggest the association of these lipid molecules with dysfunctional inflamed SAT and possibly cell cycle deregulation.

In summary, lipidomic and mRNA expression analysis of SAT revealed different content of PUFA-TAGs and MUFA-PLs in FDR participants and two genes (*LOX* and *CCND1*), which were associated with visceral adiposity and IR of the participants.

DISCUSSION

Several studies have suggested that SAT hypertrophy in FDR individuals of patients with T2DM is based on a limited capacity for

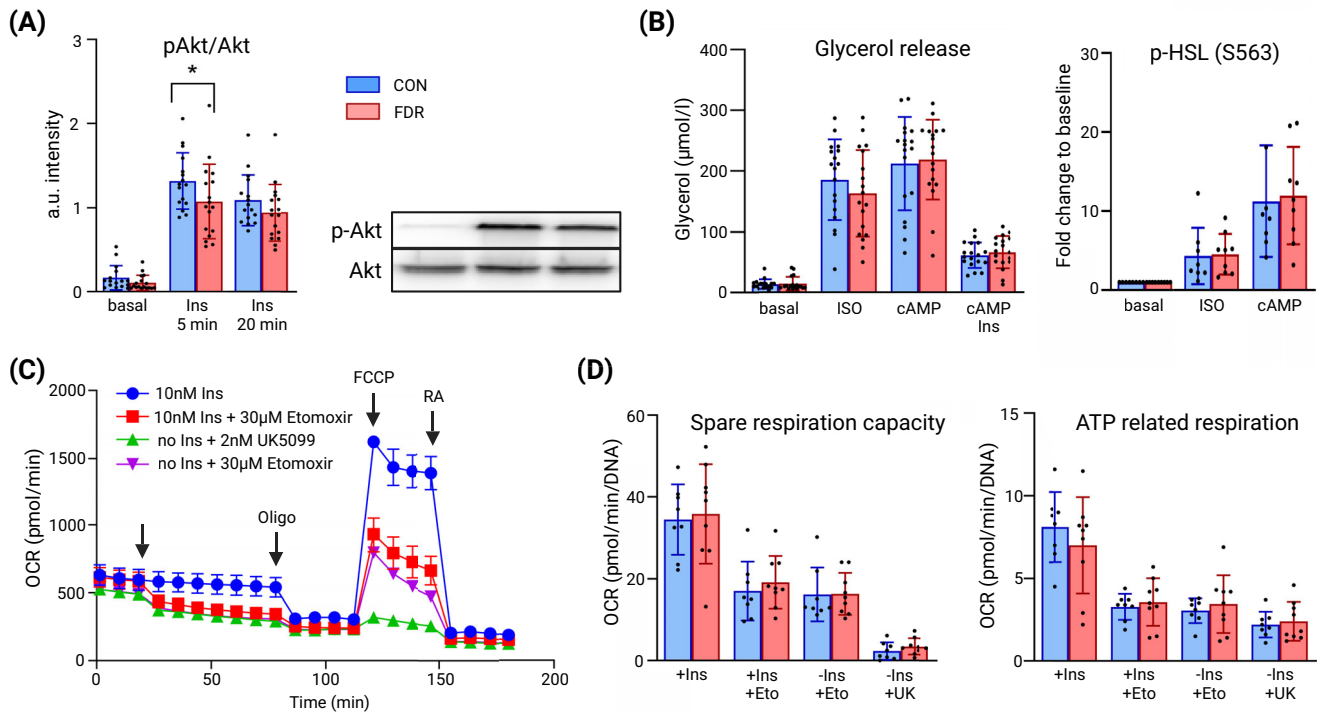


FIGURE 4 Metabolic activity of differentiated adipocytes: (A) protein kinase B (Akt) phosphorylation in response to 100 nM insulin after 5 and 20 min (control [CON] [$n = 16$]; first-degree relatives [FDR] [$n = 17$]), $*p < 0.05$, unpaired t test of log-transformed data. (B) Lipolysis: glycerol release from differentiated adipocytes in response to lipolytic (isoproterenol [ISO], 8-bromoadenosine 3',5'-cAMP) and antilipolytic (100 nM insulin) stimuli (CON [$n = 18$]; FDR [$n = 18$], technical duplicates); hormone-sensitive lipase (HSL) phosphorylation in response to lipolytic stimuli (ISO: 1 μ M isoproterenol; cAMP: 1 mM 8-bromoadenosine 3',5'-cAMP [8-bromo-cAMP]; CON [$n = 8$]; FDR [$n = 9$]). (C) The Seahorse assay-mito stress test: scheme of oxygen consumption rate (OCR) in adipocytes treated with 10 nM insulin (Ins), UK5099 (UK; inhibitor of pyruvate transport into mitochondria), and etomoxir (Eto; inhibitor of transport of long-chain fatty acids into mitochondria); representative figure, $n = 5$). (D) Difference in ATP-related respiration and spare respiration capacity in FDR vs. CON participants (CON [$n = 8$]; FDR [$n = 9$], technical pentaplicates). Data are expressed as individual points and mean \pm SD. [Color figure can be viewed at wileyonlinelibrary.com]

adipogenesis [10, 11]. However, the clear evidence that this dysfunction is one of the primary inherited features facilitating T2DM development in FDR individuals and, as such, is present before the AT accumulation, is still missing.

Reduced capacity for adipogenesis has been suggested in FDR individuals due to the presence of hypertrophic AT [5, 10]. We did not observe a significant increase in hypertrophic adipocytes in FDR individuals; however, a certain shift in relative frequency in adipocyte size was seen. The similarity in adipocyte profile with CON participants may be due to a rigorous selection of male individuals without obesity based not only on BMI but also relative FM; for this reason, we excluded male individuals with FM greater than 25% even though the BMI was less than 30. Although the two groups of male individuals did not differ in relative FM, FDR participants had higher amounts of visceral fat. This higher deposition of ectopic fat in FDR individuals is in agreement with previous studies [24, 25]. The amount of visceral region is of special interest because of its known association with metabolic disturbances such as IR and metabolic syndrome [26]. Indeed, our male FDR individuals also showed impaired glucose homeostasis and IS. It is noteworthy that we do not see a difference in glucose disposal in euglycemic clamp (reflecting comparable muscle IS) in FDR and CON participants, although IS appears to be impaired

by OGTT-derived indices and fasting glucose levels, suggesting hepatic IR. According to a study in mice fed a high-fat diet, hepatic IR precedes skeletal muscle IR and AT IR [27]. Selective liver and muscle IR phenotypes have also been described in humans with obesity [28]. Therefore, we can hypothesize that, whereas in a basal, nonstimulated state, there are signs of IR in suppression of hepatic glucose output in FDR individuals, muscle IS is probably maintained. The difference between groups in OGTT-derived indices (Matsuda and Stumvoll) is consistent with this hypothesis because lower insulinemia in 120-min OGTT may have not sufficiently suppress hepatic glucose output, whereas supraphysiological insulin levels in the clamp fully inhibited endogenous glucose production. This again points to a possible hepatic IR in FDR individuals. Based on the Adipo-IR index, AT IR is not different between the groups.

In contrast to previous evidence, we found that the intrinsic adipogenic potential of SAT cells does not appear to be impaired in male FDR individuals. This finding does not support the original hypothesis based on several studies that have shown increased hypertrophy of AT in FDR individuals [5, 10, 11]. Our results also differ from recent studies [16, 29] that have demonstrated a lower differentiation capacity of APCs from FDR individuals without obesity compared with healthy control individuals, as well as different APC transcriptome in

these groups of individuals. A limitation of our study is that we measured the expression of only predefined probes designed to cover a portion of the 97 genes of the entire APC transcriptome, which has

been instead analyzed in the previous studies. However, the participants in these studies had generally higher FM (27% ± 7%) than individuals in our study (FM 19% ± 4%). Because the degree of adiposity

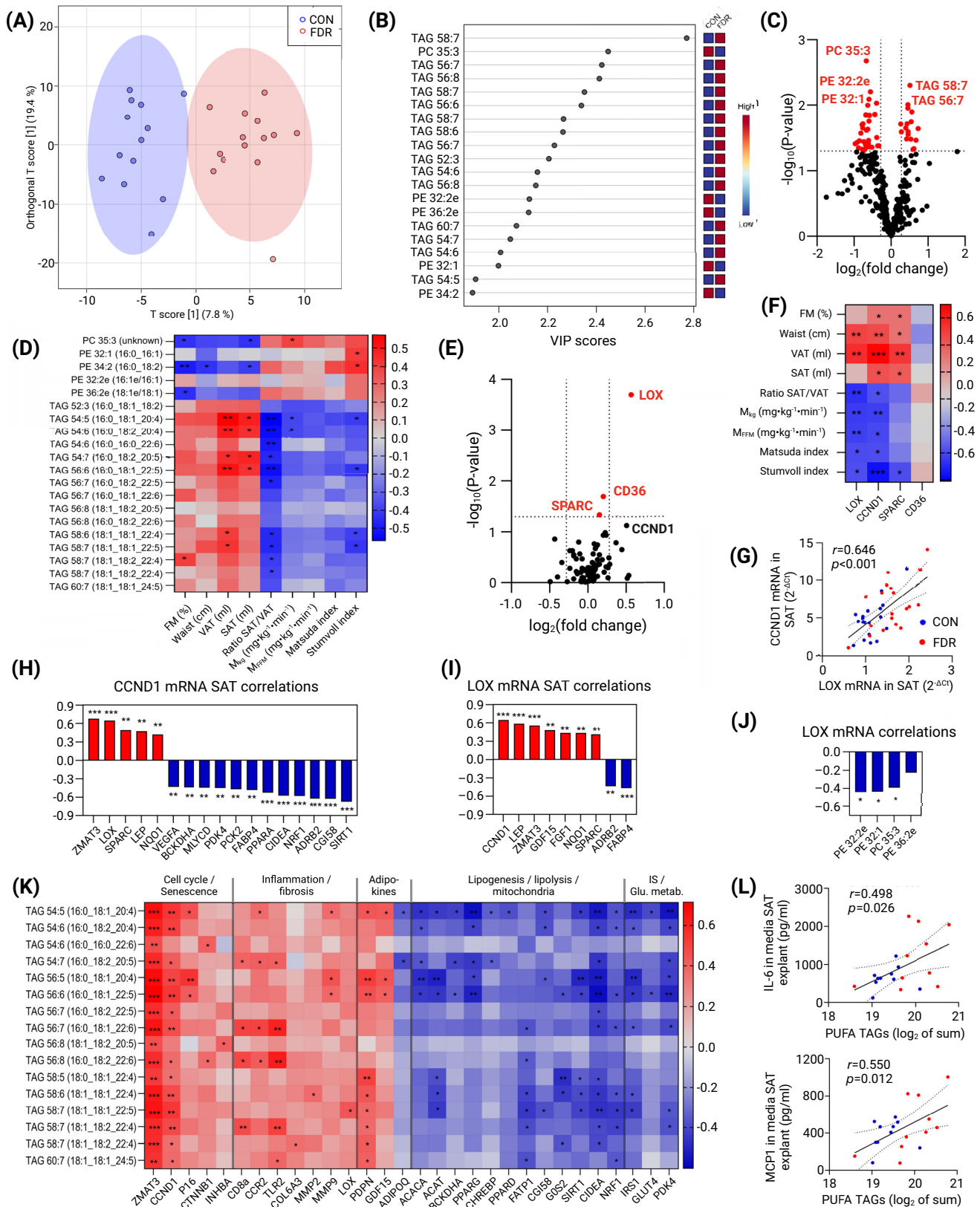


FIGURE 5 Legend on next page.

seems to play a very important role in adipogenic capacity [30], difference in FM of participants could play a role in the observed disparity. In addition, the discrepancy may be due to the sex of the participants or the composition of the differentiation medium (we used serum free media in our experiments because FBS may interfere with adipogenic conversion of cells) [31]. Taken together, we hypothesize that reduced adipogenesis and adipocyte hypertrophy in FDR individuals are not present as long as the lean phenotype is sustained but occurs with a modest increase in FM and earlier than in the general population [10, 11].

Additionally, the testing of metabolic functions of in vitro differentiated adipocytes revealed no marked differences between the groups except for Akt phosphorylation. Given that previous studies have shown impaired AT metabolism in patients with diabetes, specifically lipolysis and metabolic flexibility [32, 33], it seems likely that these disturbances also occur later, during IS worsening, and are linked with obesity onset. The only functional parameter that is different in the cells of FDR individuals, Akt phosphorylation, suggests a slower insulin signaling pathway. Because the antilipolytic effect of insulin is not affected by this altered Akt signaling, the effect on other adipocyte functions is questionable and should be verified in future studies.


Taken together, our in vitro data suggest that dysfunctional AT in predisposed men is likely to develop in association with microenvironment and external stimuli. Thus, to get more insight into SAT characteristics and hyperplastic expandability in vivo, we focused on its inflammatory, lipidomic, and mRNA expression profile. Within the lipidomic profile, we found a difference in PUFA-TAG and MUFA-PL content in SAT from FDR individuals. PUFA-TAGs are of great interest because they have been identified in a recent AT lipidome study as being fundamentally associated with the obesity phenotype [34]. In cancer cell lines and hepatocytes, they have been shown to accumulate in response to cell apoptosis downstream of p53 activation [35]. PUFA-TAGs likely play a role in a compensatory mechanism protecting the membrane from the lipoperoxidation and subsequent membrane damage. PUFA-TAG levels also correlated in our cohort with secreted proinflammatory cytokines and with *ZMAT3* and *CCND1* mRNA levels in SAT, which would support a link to adipose inflammatory/cellular stress. PUFA-TAG content was also strongly correlated with amount of VAT and the SAT/VAT ratio, suggesting that accumulation of these lipids reflect the accumulation of ectopic fat.

On the other hand, the levels of several MUFA-PLs that were reduced in FDR individuals correlated negatively with adiposity, but not with selective accumulation of visceral fat (SAT/VAT ratio). The composition of these phospholipids could be related to changes in membrane structure. The type of fatty acids in membranes has been shown to affect both their fluidity and their structure, such as the arrangement of microdomains, which, in turn, affects transport and signaling [36]. The composition of phospholipids also affects the susceptibility to lipid peroxidation [37]. Thus, it seems likely that membrane structure changes in FDR individuals as an adaptive mechanism in association with increases in FM and/or cellular stress.

At the mRNA expression level, *LOX* came out as a gene that is significantly different between FDR and CON participants, even after correction for multiple testing. *LOX* is an enzyme responsible for collagen cross-linking and thereby influences extracellular matrix stiffness and fibrosis [38]. Therefore, this finding is in agreement with the results of a previous study showing higher expression of profibrotic genes in FDR individuals [5]. Enhanced *LOX* expression in SAT of individuals who are metabolically unhealthy seems to be detrimental [39], and it decreases with weight loss [40]. We did not test which cell type is responsible for the increased *LOX* expression in FDR individuals. Nevertheless, we did not see a difference in the *LOX* expression in adipocytes in vitro, and a recent study showed that *LOX* expression is increased by proinflammatory stimuli specifically in macrophages, which action mediates stiffness of the microenvironment and affects adipocyte function [41]. Furthermore, *LOX* overexpression in murine vascular smooth muscle cells enhanced oxidative stress and caused mitochondrial dysfunction [42]. Even in our study, *LOX* mRNA correlated strongly with *ZMAT3*, *CCND1*, *NOQ1*, *FGF1*, and *GDF15* in SAT, suggesting an association with cellular and oxidative stress [43–45]. Importantly, these genes are associated with the p53 pathway [43, 46], which responds to stress signals by regulating DNA repair, cell cycle arrest, cell death, or senescence. *ZMAT3* and *CCND1* were also shown to participate in senescent phenotype of adipose cells and limit adipogenesis [16, 47, 48]. This, together with the findings from lipidomics, led us to hypothesize that cellular stress associated with cell cycle deregulation may be a part of predisposition to T2DM. An overexpression or downregulation of *LOX*, specifically in SAT APC or macrophages, could provide direct evidence of the functional association among *LOX*, AT expandability, and susceptibility to T2DM development.

FIGURE 5 Lipidomic and mRNA expression analysis of subcutaneous adipose tissue (SAT). (A) Orthogonal partial least square - discriminant analysis of lipidome (control [CON] [$n = 13$]; first-degree relatives [FDR] [$n = 14$]). (B) Variable importance in projection (VIP) score of most differing lipid molecules in FDR and CON participants (CON [$n = 13$]; FDR [$n = 14$]). (C) Volcano plot of lipidome (CON [$n = 13$]; FDR [$n = 14$]). (D) Correlation heat map of 20 most differing lipid molecules (polyunsaturated fatty acids in triacylglycerols [PUFA-TAGs], phospholipids [PLs]) with adiposity and insulin sensitivity (IS; color mapping: Pearson correlation coefficient; CON [$n = 12$ –13]; FDR [$n = 13$ –14]). (E) Volcano plot of mRNA expression ($p < 0.05$ marked in red, Mann-Whitney U test; CON [$n = 19$]; FDR [$n = 19$]). (F) Correlation heat map of lysyl oxidase (*LOX*), cyclin D1 (*CCND1*), *CD36*, and secreted protein acidic and rich in cysteine (*SPARC*) genes with adiposity and IS parameters (color mapping: Pearson correlation coefficient; CON [$n = 18$ –19]; FDR [$n = 16$ –19]). (G) Correlations of *LOX* and *CCND1* mRNA (CON [$n = 19$]; FDR [$n = 19$]). (H) Correlations of *CCND1* mRNA with gene expression in SAT (CON [$n = 18$ –19]; FDR [$n = 19$]). (I) Correlations of *LOX* mRNA with gene expression in SAT (CON [$n = 18$ –19]; FDR [$n = 19$]). (J) Correlations of *LOX* mRNA with with PLs in SAT (CON [$n = 13$]; FDR [$n = 14$]). (K) Correlation heat map of PUFA-TAGs with mRNA expression in SAT (color mapping: Pearson correlation coefficient; CON [$n = 11$ –13]; FDR [$n = 11$ –14]). (L) Correlation of PUFA-TAGs with IL-6 and monocyte chemoattractant protein-1 (MCP-1) secretion from SAT explants (CON [$n = 10$]; FDR [$n = 10$]). Pearson correlation coefficients are shown for all the correlations, * $p < 0.05$, ** $p < 0.01$, *** $p < 0.001$. [Color figure can be viewed at wileyonlinelibrary.com]

Despite the comprehensiveness of this study, it has several limitations. In order to achieve the greatest possible homogeneity of the groups, we recruited only male individuals; therefore, we cannot exclude the influence of sex on the observed parameters. Furthermore, we analyzed only SAT, whereas VAT amount in our study was more so affected by family predisposition to T2DM than SAT. VAT acquisition (surgery) in healthy participants in our study was not part of the protocol because of ethical issues. Nevertheless, because adipocyte size, SVF cell number, and gene expression are strongly correlated in VAT and SAT [49, 50], it can be assumed that VAT metabolism, morphology, and other characteristics are reflected closely by SAT characteristics. Finally, our results are mostly associative; therefore, functional studies should be warranted in this issue.

Considering all of our observations, it can be summarized that the intrinsic adipogenic capacity of APCs seems to be preserved in relatives of patients with T2DM before FM accumulation. Importantly, PUFA-TAG levels and mRNA expression in SAT of predisposed male individuals may indicate an increased level of cellular stress and cell cycle deregulation, which may point to AT dysfunction during the onset of obesity. Our study also revealed PUFA-TAGs and LOX expression in SAT as markers of impaired IS and VAT accumulation in male individuals without obesity. Thus, these molecules may play a role in the pathophysiology and inheritance of T2DM, and we propose them as important target for future research in this area. 

AUTHOR CONTRIBUTIONS

Michaela Šiklová, Jan Gojda, and Lenka Rossmeislová designed and coordinated the research. Michaela Šiklová performed statistical analysis and wrote the manuscript. Veronika Šrámková, Michal Koc, Terezie Čížková, Barbora Ondrůjová, Zuzana Varaliová, Ondrej Kuda, Jana Neubert, Marek Wilhelm, and Moustafa Elkalaf conducted in vitro and ex vivo research. Eva Krauzová, Jan Gojda, and Lukáš Lambert conducted clinical investigations. All authors contributed to the analysis and interpretation of data and critically revised and approved the final manuscript. Michaela Šiklová is a guarantor of this work and, as such, had full access to all of the data in the study and takes responsibility for the integrity of the data and the accuracy of the data analysis.

ACKNOWLEDGMENTS

The authors would like to thank Jana Potočková and Lenka Beranová for excellent technical assistance; Pavel Cejnar for consultation of statistical analysis; and Marek Štěpán and Vladimír Štich for clinical investigation of the participants. The authors would also like to acknowledge the Metabolomics Core Facility at the Institute of Physiology, Czech Academy of Sciences (Tomáš Čajka) for lipidomics profiling.

CONFLICT OF INTEREST STATEMENT

Jan Gojda reports European Foundation for the Study of Diabetes (EFSD) Mentorship program supported by AstraZeneca plc. The other authors declared no conflict of interest.

DATA AVAILABILITY STATEMENT

Data generated during this study are available from the corresponding author upon reasonable request.

ORCID

Michaela Šiklová  <https://orcid.org/0000-0003-0489-1069>

Terezie Čížková  <https://orcid.org/0000-0001-7565-2984>

REFERENCES

- Saeedi P, Petersohn I, Salpea P, et al. Global and regional diabetes prevalence estimates for 2019 and projections for 2030 and 2045: results from the International Diabetes Federation Diabetes Atlas, 9th edition. *Diabetes Res Clin Pract.* 2019;157:107843.
- InterAct C, Scott RA, Langenberg C, et al. The link between family history and risk of type 2 diabetes is not explained by anthropometric, lifestyle or genetic risk factors: the EPIC-InterAct study. *Diabetologia.* 2013;56:60-69.
- Bays HE, Chapman RH, Grandy S, Group SI. The relationship of body mass index to diabetes mellitus, hypertension and dyslipidaemia: comparison of data from two national surveys. *Int J Clin Pract.* 2007;61:737-747.
- Guilherme A, Virbasius JV, Puri V, Czech MP. Adipocyte dysfunctions linking obesity to insulin resistance and type 2 diabetes. *Nat Rev Mol Cell Biol.* 2008;9:367-377.
- Henninger AM, Eliasson B, Jenndahl LE, Hammarstedt A. Adipocyte hypertrophy, inflammation and fibrosis characterize subcutaneous adipose tissue of healthy, non-obese subjects predisposed to type 2 diabetes. *PLoS One.* 2014;9:e105262.
- Alligier M, Gabert L, Meugnier E, et al. Visceral fat accumulation during lipid overfeeding is related to subcutaneous adipose tissue characteristics in healthy men. *J Clin Endocrinol Metab.* 2013;98:802-810.
- Levtel E, Pavlides M, Banerjee R, et al. Ectopic and visceral fat deposition in lean and obese patients with type 2 diabetes. *J Am Coll Cardiol.* 2016;68:53-63.
- Isakson P, Hammarstedt A, Gustafson B, Smith U. Impaired preadipocyte differentiation in human abdominal obesity: role of Wnt, tumor necrosis factor-alpha, and inflammation. *Diabetes.* 2009;58:1550-1557.
- Weyer C, Foley JE, Bogardus C, Tataranni PA, Pratley RE. Enlarged subcutaneous abdominal adipocyte size, but not obesity itself, predicts type II diabetes independent of insulin resistance. *Diabetologia.* 2000;43:1498-1506.
- Arner P, Arner E, Hammarstedt A, Smith U. Genetic predisposition for type 2 diabetes, but not for overweight/obesity, is associated with a restricted adipogenesis. *PLoS One.* 2011;6:e18284.
- Smith U, Kahn BB. Adipose tissue regulates insulin sensitivity: role of adipogenesis, de novo lipogenesis and novel lipids. *J Intern Med.* 2016;280:465-475.
- Gustafson B, Gogg S, Hedjazifar S, Jenndahl L, Hammarstedt A, Smith U. Inflammation and impaired adipogenesis in hypertrophic obesity in man. *Am J Physiol Endocrinol Metab.* 2009;297:E999-E1003.
- Virtue S, Vidal-Puig A. Adipose tissue expandability, lipotoxicity and the metabolic syndrome—an allostatic perspective. *Biochim Biophys Acta.* 2010;1801:338-349.
- Barbagallo I, Li Volti G, Galvano F, et al. Diabetic human adipose tissue-derived mesenchymal stem cells fail to differentiate in functional adipocytes. *Exp Biol Med (Maywood).* 2017;242:1079-1085.
- Gustafson B, Nerstedt A, Smith U. Reduced subcutaneous adipogenesis in human hypertrophic obesity is linked to senescent precursor cells. *Nat Commun.* 2019;10:2757.
- Spinelli R, Florese P, Parrillo L, et al. ZMAT3 hypomethylation contributes to early senescence of preadipocytes from healthy first-degree relatives of type 2 diabetics. *Aging Cell.* 2022;21:e13557.

17. Cizkova T, Stepan M, Dadova K, et al. Exercise training reduces inflammation of adipose tissue in the elderly: cross-sectional and randomized interventional trial. *J Clin Endocrinol Metab.* 2020;105:e4510-e4526.
18. Matsuda M, DeFronzo RA. Insulin sensitivity indices obtained from oral glucose tolerance testing: comparison with the euglycemic insulin clamp. *Diabetes Care.* 1999;22:1462-1470.
19. Stumvoll M, Van Haeften T, Fritsche A, Gerich J. Oral glucose tolerance test indexes for insulin sensitivity and secretion based on various availabilities of sampling times. *Diabetes Care.* 2001;24:796-797.
20. Lambert L, Novak M, Siklova M, Krauzova E, Stich V, Burgetova A. Hybrid and model-based iterative reconstruction influences the volumetry of visceral and subcutaneous adipose tissue on ultra-low-dose CT. *Obesity (Silver Spring).* 2020;28:2083-2089.
21. Brezinova M, Cajka T, Oseeva M, et al. Exercise training induces insulin-sensitizing PAHSAs in adipose tissue of elderly women. *Biochim Biophys Acta Mol Cell Biol Lipids.* 2020;1865:158576.
22. Lawler HM, Underkofler CM, Kern PA, Erickson C, Bredbeck B, Rasouli N. Adipose tissue hypoxia, inflammation, and fibrosis in obese insulin-sensitive and obese insulin-resistant subjects. *J Clin Endocrinol Metab.* 2016;101:1422-1428.
23. van Harmelen V, Skurk T, Rohrig K, et al. Effect of BMI and age on adipose tissue cellularity and differentiation capacity in women. *Int J Obes Relat Metab Disord.* 2003;27:889-895.
24. Cederberg H, Stancakova A, Kuusisto J, Laakso M, Smith U. Family history of type 2 diabetes increases the risk of both obesity and its complications: is type 2 diabetes a disease of inappropriate lipid storage? *J Intern Med.* 2015;277:540-551.
25. Nyholm B, Nielsen MF, Kristensen K, et al. Evidence of increased visceral obesity and reduced physical fitness in healthy insulin-resistant first-degree relatives of type 2 diabetic patients. *Eur J Endocrinol.* 2004;150:207-214.
26. Bergman RN, Kim SP, Catalano KJ, et al. Why visceral fat is bad: mechanisms of the metabolic syndrome. *Obesity (Silver Spring).* 2006;14(Suppl 1):165-195.
27. Turner N, Kowalski GM, Leslie SJ, et al. Distinct patterns of tissue-specific lipid accumulation during the induction of insulin resistance in mice by high-fat feeding. *Diabetologia.* 2013;56:1638-1648.
28. Vogelzangs N, van der Kallen CJH, van Greevenbroek MMJ, et al. Metabolic profiling of tissue-specific insulin resistance in human obesity: results from the Diogenes study and the Maastricht study. *Int J Obes (Lond).* 2020;44:1376-1386.
29. Mirra P, Desiderio A, Spinelli R, et al. Adipocyte precursor cells from first degree relatives of type 2 diabetic patients feature changes in *hsa-mir-23a-5p*, *-193a-5p*, and *-193b-5p* and insulin-like growth factor 2 expression. *FASEB J.* 2021;35:e21357.
30. Rossmeslova L, Malisova L, Kracmerova J, et al. Weight loss improves the adipogenic capacity of human preadipocytes and modulates their secretory profile. *Diabetes.* 2013;62:1990-1995.
31. Skurk T, Ecklebe S, Hauner H. A novel technique to propagate primary human preadipocytes without loss of differentiation capacity. *Obesity (Silver Spring).* 2007;15:2925-2931.
32. Baker NA, Muir LA, Washabaugh AR, et al. Diabetes-specific regulation of adipocyte metabolism by the adipose tissue extracellular matrix. *J Clin Endocrinol Metab.* 2017;102:1032-1043.
33. Smith RL, Soeters MR, Wust RCI, Houtkooper RH. Metabolic flexibility as an adaptation to energy resources and requirements in health and disease. *Endocr Rev.* 2018;39:489-517.
34. Lange M, Angelidou G, Ni Z, et al. AdipoAtlas: a reference lipidome for human white adipose tissue. *Cell Rep Med.* 2021;2:100407.
35. Li N, Lizardo DY, Atilla-Gokcumen GE. Specific triacylglycerols accumulate via increased lipogenesis during 5-FU-induced apoptosis. *ACS Chem Biol.* 2016;11:2583-2587.
36. Ibarguren M, Lopez DJ, Escriba PV. The effect of natural and synthetic fatty acids on membrane structure, microdomain organization, cellular functions and human health. *Biochim Biophys Acta.* 2014;1838:1518-1528.
37. Rodencal J, Dixon SJ. A tale of two lipids: lipid unsaturation commands ferroptosis sensitivity. *Proteomics.* 2023;23:e2100308.
38. Vallet SD, Ricard-Blum S. Lysyl oxidases: from enzyme activity to extracellular matrix cross-links. *Essays Biochem.* 2019;63:349-364.
39. Sotak M, Rajan MR, Clark M, et al. Healthy subcutaneous and omental adipose tissue is associated with high expression of extracellular matrix components. *Int J Mol Sci.* 2022;23:520.
40. Liu Y, Aron-Wisnewsky J, Marcelin G, et al. Accumulation and changes in composition of collagens in subcutaneous adipose tissue after bariatric surgery. *J Clin Endocrinol Metab.* 2016;101:293-304.
41. Huang A, Lin YS, Kao LZ, et al. Inflammation-induced macrophage lysyl oxidase in adipose stiffening and dysfunction in obesity. *Clin Transl Med.* 2021;11:e543.
42. Martinez-Revelles S, Garcia-Redondo AB, Avendano MS, et al. Lysyl oxidase induces vascular oxidative stress and contributes to arterial stiffness and abnormal elastin structure in hypertension: role of p38MAPK. *Antioxid Redox Signal.* 2017;27:379-397.
43. Bersani C, Xu L, Vilborg A, Lui W, Wiman KG. Correction to: Wig-1 regulates cell cycle arrest and cell death through the p53 targets FAS and 14-3-3s. *Oncogene.* 2023;42:709.
44. Gasser E, Sancar G, Downes M, Evans RM. Metabolic messengers: fibroblast growth factor 1. *Nat Metab.* 2022;4:663-671.
45. Patel S, Alvarez-Guaita A, Melvin A, et al. GDF15 provides an endocrine signal of nutritional stress in mice and humans. *Cell Metab.* 2019;29(3):707-718.e8.
46. Zhao R, Liu W, Wang M, et al. Lysyl oxidase inhibits TNF-alpha induced rat nucleus pulposus cell apoptosis via regulating Fas/FasL pathway and the p53 pathways. *Life Sci.* 2020;260:118483.
47. Fu M, Rao M, Bouras T, et al. Cyclin D1 inhibits peroxisome proliferator-activated receptor gamma-mediated adipogenesis through histone deacetylase recruitment. *J Biol Chem.* 2005;280:16934-16941.
48. Li Q, Hagberg CE, Silva Cascales H, et al. Obesity and hyperinsulinemia drive adipocytes to activate a cell cycle program and senescence. *Nat Med.* 2021;27:1941-1953.
49. Belligoli A, Compagnin C, Sanna M, et al. Characterization of subcutaneous and omental adipose tissue in patients with obesity and with different degrees of glucose impairment. *Sci Rep.* 2019;9:11333.
50. Klimcakova E, Roussel B, Kovacova Z, et al. Macrophage gene expression is related to obesity and the metabolic syndrome in human subcutaneous fat as well as in visceral fat. *Diabetologia.* 2011;54:876-887.

SUPPORTING INFORMATION

Additional supporting information can be found online in the Supporting Information section at the end of this article.

How to cite this article: Šiklová M, Šrámková V, Koc M, et al. The role of adipogenic capacity and dysfunctional subcutaneous adipose tissue in the inheritance of type 2 diabetes mellitus: cross-sectional study. *Obesity (Silver Spring).* 2024;32(3):547-559. doi:10.1002/oby.23969